Chevron Defect at the Intersection of Grain Boundaries with Free Surfaces in Au

T. Radetic, F. Lançon,* and U. Dahmen
National Center for Electron Microscopy, LBNL, Berkeley, California 94720
(Received 17 May 2002; published 1 August 2002)

We have identified a new defect at the intersection between grain boundaries and surfaces in Au using atomic resolution transmission electron microscopy. At the junction line of 90° ⟨110⟩ tilt grain boundaries of (110)-(001) orientation with the free surface, a small segment of the grain boundary, about 1 nm in length, dissociates into a triangular region with a chevronlike stacking disorder and a distorted hcp structure. The structure and stability of these defects are confirmed by atomistic simulations, and we point out the relationship with the one-dimensional incommensurate structure of the grain boundary.

DOI: 10.1103/PhysRevLett.89.085502 PACS numbers: 61.72.Dd, 61.50.Ks, 61.72.Mm, 81.30.Hd

The atomic structure of solids at surfaces and interfaces is often found to be significantly different from the bulk. The best-known example of this difference is the 7×7 reconstruction of the Si {111} surface [1]. Surface reconstruction and its dependence on crystallographic and thermodynamic variables has been studied extensively, and the phenomenon is now well-established for many types of solids (e.g., [2]). Interfaces between solid phases display similar phenomena, but much less is known about their behavior because experimental techniques for the study of interfaces are much more limited than for surfaces. At interfaces, atomic relaxation can take a number of different forms, including emission of partial dislocations [3] and formation of extended structures, or dissociation [4–6]. Dissociation is often found at grain boundaries in low stacking fault materials such Ag, Au, Ni, Si, and Cu, when a single planar interface is ''wetted'' by a solid layer with a different orientation and sometimes with a different structure. For example, certain grain boundaries in face centered cubic (fcc) Cu are found to form a thin layer with the $9R$ structure [7–9] or even the body centered cubic (bcc) structure [10].

In this work, we have studied the atomic structure at the junction of 90° ⟨110⟩ tilt grain boundaries with the free surface in Au using high resolution transmission electron microscopy. This type of configuration is of interest because structural relaxation at line junctions [11] can affect the morphological evolution of thin films by controlling the stability of particular boundary inclinations or by forming surface grooves that pin the boundary and prevent grain growth [12].

It is well known that the dependence of interface phenomena on crystallographic parameters is more complex than for surfaces, because they vary with the orientation of the interface as well as the orientation relationship between the two crystals. To describe the intersection of a grain boundary with a surface requires at least seven parameters. To study the effect experimentally, we chose thin films of Au with the mazed bicrystal structure [13]. Such films are characterized by a random distribution of many grains in only two orientations, related to each other by a 90° rotation around a common ⟨110⟩ axis. As grain boundaries tend to be normal to the film surface, i.e., parallel to the common ⟨110⟩ axis, all boundaries are of pure tilt type, and their crystallography is described by a $\Sigma 99$ 90° ⟨110⟩ tilt character. Of the five macroscopic parameters that describe a general grain boundary, only one is variable in this geometry (the boundary inclination, which can range from 0 to 2π). Grains envelop each other, forming a convoluted, mazelike structure that presents all possible grain boundary inclinations in a single sample. The morphology is that of a Potts model microstructure with degeneracy 2, equivalent to an Ising model [14,15].

Mazed bicrystal films of Au in {110} orientation were grown by physical vapor deposition on {001} Ge substrates [16,17]. Films for characterization by high resolution electron microscopy (HREM) were approximately 10 nm thick and contained a number of holes. Where grain boundaries intersected these holes, the grain boundary junctions with the free surface could be studied directly by HREM. An analysis of the distribution of grain boundary orientations measured over large areas of the thin films indicated a clear anisotropy, manifested in a preference for certain orientations or facets of the interface [16]. At the {110}/{100} facet, (001) planes from one grain meet (011) planes from the other grain edge to edge, and, as their interplanar spacings are in a ratio of $1/\sqrt{2}$, the interface is incommensurate in one direction [18]. This boundary has been studied previously by high resolution electron microscopy and atomistic simulations [19–21]. In the present Letter, we report that, at the intersection of the {110}/{100} facet with the free surface, the grain boundary relaxes by dissociation into a characteristic triangular defect. These observations are compared with atomistic simulations.

HREM images of typical intersections are shown in Figs. 1(a) and 1(b). A straight {110}/{100} incommensurate grain boundary facet extends toward the free surface, and, close to the intersection, the boundary dissociates into a triangular region with a characteristic defect structure. The undissociated grain boundary lies exactly parallel to (100) planes in the left grain and to (110) planes in the right grain. Its core structure consists of fairly open structural

 © 2002 The American Physical Society

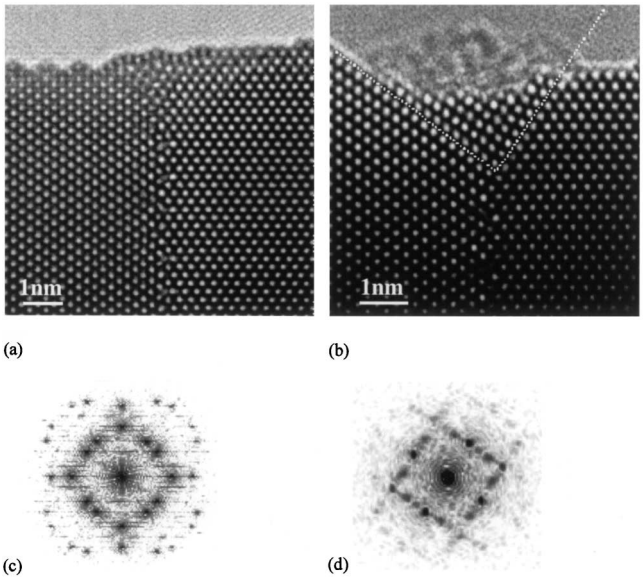

FIG. 1. Atomic resolution transmission electron micrographs of chevron defects at the intersection of the 90° ⟨110⟩ tilt grain boundary with the free surface [(a),(b)]. The triangular region of dissociation is marked by dashed lines in (b). The boundaries of the defect are parallel to {111} planes in both grains. Inside the defect, there are stacking faults on alternate layers resulting in a local hcp stacking sequence. The Fourier diffractograms in (c) and (d) illustrate the difference between the undissociated boundary (c) and the chevron defect in the dissociated boundary (d).

units [21]. At the Y-shaped dissociation near the surface, the boundary splits into two interfaces parallel to {111} planes in the two grains. As a result of the 90° tilt character of the bicrystal, the two corresponding {111} planes in the two crystals enclose a 90° angle such that the defect shape approximates a right triangle. The enclosed region is characterized by a stacking disorder of the two sets of close-packed planes that lie parallel to the two mutually perpendicular {111} interfaces, giving it the appearance of a chevron pattern.

Our observations indicate that the {110}/{001} inclination of the $\Sigma 99$ ⟨110⟩ tilt boundary in Au dissociates if it intersects the surface at an angle of $90° \pm 30°$. Of the more than 30 grain boundaries with the same {110}/{001} inclination investigated in this work, all but one exhibited the chevron defect. The size of the defect, measured as the length of the boundary transformed by dissociation, was found to be in the range 0.6–1.7 nm. The defect appeared in both, annealed and unannealed, samples. Its characteristic atomic structure is analyzed below.

The defect shown in Fig. 1(a) exhibits stacking faults on alternate {111} planes, forming thin segments with hcp stacking sequence. The different atomic structure of the dissociated defect region is also reflected in the structure of the free surface. In high vacuum, Au crystals with perfect fcc structure exhibit surface reconstruction with steps parallel to {111} or {100} planes. This can be seen directly in Fig. 1(a), where the left grain exhibits a typical "missing row" 1×2 and 1×3 reconstruction of the {110} surface [22,23], and the right grain shows atomically flat {100} terraces. However, in the defect region, the surface is less faceted and less crystallographically ordered. The atomic arrangement in the central part of the defect is usually highly distorted, and no typical unit cell is apparent. The structure tends to maintain close-packed planes parallel to the two {111} interfaces, though their stacking sequence varies within a defect and from one defect to another.

A quantitative description that is sensitive to interplanar spacing and stacking disorder but independent of the precise stacking sequence is given by the Fourier transforms shown in Figs. 1(c) and 1(d). The Fourier transform of the grain boundary structure in Fig. 1(c) shows the two single crystal diffraction patterns in ⟨110⟩ orientation rotated 90° relative to each other as well as streaks normal to the interface that are due to the incommensurate boundary structure itself [21]. By comparison, the Fourier transform of the chevron defect [Fig. 1(d)] shows a square pattern made of four spots of intensity, normal to the close-packed planes in the two grains. Streaks of intensity perpendicular to the four spots are due to the stacking disorder of the close-packed planes, and the intensity modulation around the spots indicates the statistical distribution of stacking faults. The absence of diffraction intensity outside the square pattern shows that the defect maintains a nearly crystalline atomic arrangement with first and second neighbor distances corresponding to those typical for fcc and hcp or polytype stacking. The comparison with the Fourier transform of the undissociated grain boundary illustrates how the transformation can be envisaged as a statistical reordering of two mutually perpendicular sets of close-packed planes that eliminates the 002 reflections (characteristic of the fcc structure) while maintaining the 111 reflections (due to the close-packed planes).

In order to understand these observations, we conducted atomistic simulations for the same geometry. Previous calculations successfully predicted the observed incommensurate structure of {110}/{001} boundaries in Au [21]. The same method was used here to simulate the intersection of the grain boundary with the free surface. Based on tight-binding second moment approximation [24], the atomic interactions are represented by an N-body potential, which has been used to study the stability of noble metal surfaces [25]. The potential parameters for gold were fitted [26] to the cohesive energy, the lattice parameter, and the elastic constants. The vacancy formation energy and the Rose curve are well reproduced. Because of the functional form of the potential similar to EAM potentials [5], the stacking fault energy is underestimated (1.5 mJ/m^2 compared to an experimental value of 32 mJ/m^2). To obtain an atomic model of the chevron defect, a starting configuration was derived from the experimental high resolution micrograph in Fig. 1(b).

The x and y coordinates correspond to the location of the maximum intensity of the spots while the z coordinates are imposed, subject to constraints of continuity for the crystalline segments. By minimizing the potential energy with respect to the atomic coordinates, the role of the simulation is to find a coherent set of atomic positions and to propose an interpretation of the defect stability from the energy distribution in the material. The relaxed structure calculated using this procedure is shown in Fig. 2(a). The corresponding multislice high resolution image simulation in Fig. 2(b) can be compared directly to the observed image in Fig. 1(b). In the model of the relaxed structure [Fig. 2(a)], energy is indicated by shading of the atoms. Atoms in the highest energy positions appear darkest in color, illustrating the high energy of the original grain boundary and the lower energy of the chevron defect. It is also apparent from the model that the structure inside the defect is more compact than in the undissociated grain boundary, and the stability of the defect can be explained qualitatively in terms of densification of the crystal at the intersection of the boundary with the free surface. The driving force for the spontaneous relaxation is the energy of the grain boundary, whose open structure has lower atomic density and lower coordination than the bulk fcc structure. Both, the experimental observations (Fig. 1) and simulated structure (Fig. 2), show that atomic arrangement inside the chevron defect is more compact than in the boundary. The mean coordination numbers n of the atoms have been calculated in the model (with a maximum neighbor distance equal to 0.31 nm). For the atoms in the first rows on each side of the interface, n is equal to 10.3, while inside the chevron region $n = 11.9$. Although the structure inside the defect is distorted, it still preserves interatomic distances and coordination similar to those in the close-packed fcc and hcp structures ($n = 12$).

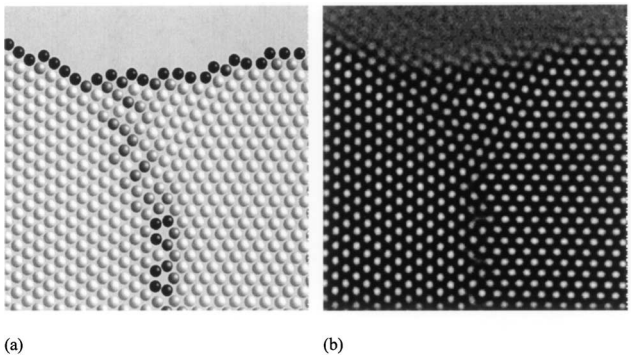

FIG. 2. (a) Atomistic simulation of relaxation of the (110)/(001) grain boundary at the free surface. Local atomic energy is indicated by shading (white for lowest energy, black for highest energy at the grain boundary). For higher energies, the color saturates to black. Atoms located at the free surface have the highest energy. (b) Multislice phase contrast image simulation for imaging conditions used in this work.

To determine its dependence on size, the defect was modeled as a triangular region with hcp stacking and the total energy of its relaxed structure was calculated. Because of the crystallographic constraints, four different configurations had to be considered for each defect, distinguished only by their translation states. The minimum energy, calculated as a function of defect size, is shown in Fig. 3. The minimum at a size of about 4–5 nm is somewhat larger than the observed range of 0.6–1.7 nm. The model is expected to overestimate the optimum defect size because it underestimates the stacking fault energy. The optimum defect size will be given by the energy balance between the savings due to the length of boundary eliminated $L\gamma_{\mathrm{gb}}$ and the cost of generating two new boundaries $2\sqrt{2}L\gamma_{\mathrm{cb}}$ plus the excess bulk energy L^2E_V of the defect structure itself. Here, γ_{gb} is the energy of the grain boundary and γ_{cb} is the energy of the interfaces bounding the chevron defect, closely related to the stacking fault energy. Thus, the total energy of a defect of size L can be approximated as $L(2\sqrt{2}\gamma_{\mathrm{cb}} - \gamma_{\mathrm{gb}}) + L^2E_V$, and a fit of this equation is shown as the dashed curve in Fig. 3, with a minimum at $L = (\gamma_{\mathrm{gb}} - 2\sqrt{2}\gamma_{\mathrm{cb}})/2E_V$.

The experimental observations indicate that different configurations of the defect are possible. This behavior is reproduced in the simulations and can be related to nature of the asymmetric {110}/{001} grain boundary, which is incommensurate in one direction and thus forms a quasiperiodic structure [21]. It is due to the latter property that

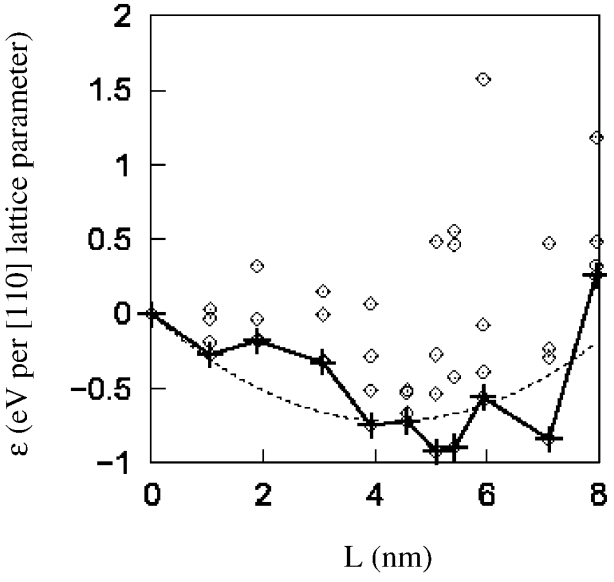

FIG. 3. Variation of defect energy with size. For each size, four different configurations were considered, and the solid line traces the lowest-energy values. The dashed line is a fit of the type $ax^2 + bx$ to these data. The calculated curve is not continuous, because there is a discrete number of configurations, and its roughness is probably due to the fact that the defect intersects (and replaces) a nonperiodic boundary.

the structure of the chevron depends on the position of the surface. The fact that there are no two identical points at the grain boundary implies that there should not be two identical chevrons. This difference can be seen in the simulations as well as in experimental images.

The dissociation of a line junction, first reported here for the intersection of a grain boundary with a surface, would be expected to be a more general phenomenon, relevant for the line intersection of any two, three, or more planar interfaces in the same zone, as found, for example, at all grain boundary triple junctions in polycrystalline materials. Insofar as dissociation of grain boundaries can be described as a wetting phenomenon, the wetting conditions for line junctions (critical angle $\pi/3$) are less stringent than those for plane junctions [27]; and, hence, the effect could be even more important for triple lines than for grain boundaries.

In summary, a novel mode of grain boundary relaxation at the intersection with a free surface has been observed. The line junction between a $\{110\}/\{001\}$ grain boundary and a surface dissociates into a defect of triangular cross section with boundaries parallel to $\{111\}$ planes in both crystals. The structure of the defect is characterized by a chevronlike stacking disorder parallel to the two interfaces and a distorted hcp region in the center of the defect. It is believed that this defect has more general importance in low stacking fault materials, influencing grain boundary mobility and, hence, coarsening of grains and the stability of thin films.

This work was supported by the Director, Office of Basic Energy Sciences, Materials Science Division, U.S. Department of Energy, under Contract No. De-AC3-76SF00098. F. L. acknowledges the hospitality of NCEM during a research leave at Berkeley Laboratory.

*Present address: Département de Recherche Fondamentale sur la Matière Condensée, SP2M, CEA, Cedex 9, 38054 Grenoble, France.

[1] K. Takayanagi, Y. Tanishiro, S. Takahashi, and M. Takahashi, Surf. Sci. **164**, 367 (1985).
[2] A. Zangwill, *Physics at Surfaces* (Cambridge University Press, Cambridge, England, 1991).
[3] J. D. Rittner, D. N. Seidman, and K. L. Merkle, Phys. Rev. B **53**, R4241 (1996).
[4] K. L. Merkle, Microsc. Microanal. **3**, 339 (1997).
[5] J. D. Rittner and D. N. Seidman, Phys. Rev. B **54**, 6999 (1996).
[6] K. L. Merkle, J. Phys. Chem. Solids **55**, 991 (1994).
[7] D. Hofmann and F. Ernst, Ultramicroscopy **53**, 205 (1994).
[8] D. L. Medlin, S. M. Foiles, G. H. Campbell, and C. B. Carter, Mater. Sci. Forum **294–296**, 35 (1999).
[9] D. L. Medlin, S. M. Foiles, and D. A. Cohen, Acta Mater. **49**, 3689 (2001).
[10] C. Schmidt, F. Ernst, M. W. Finnis, and V. Vitek, Phys. Rev. Lett. **75**, 2160 (1995).
[11] A. H. King, Interface Sci. **7**, 251 (1999).
[12] W. W. Mullins, Acta Metall. **6**, 414 (1958).
[13] U. Dahmen and K. H. Westmacott, in *Proceedings of the Materials Research Society* (Materials Research Society, Pittsburgh, 1991), Vol. 229, p. 167.
[14] P. S. Sahni *et al.*, Phys. Rev. B **28**, 2705 (1983).
[15] G. S. Grest and D. J. Srolovitz, Phys. Rev. B **30**, 5150 (1984).
[16] T. Radetic and U. Dahmen, in *Proceedings of the Materials Research Society, Boston, 2001*, edited by C. S. Ozkan, R. C. Cammarata, L. B. Freund, and H. Gao (Materials Research Society, Pittsburgh, 2001), Vol. 695.
[17] K. H. Westmacott, S. Hinderberger, and U. Dahmen, Philos. Mag. A **81**, 1547 (2001).
[18] A. P. Sutton, Acta Metall. **36**, 1291 (1988).
[19] P. A. Deymier, M. Shamsuzzoha, and J. D. Weinberg, J. Mater. Res. **6**, 1461 (1991).
[20] J. M. Penisson, F. Lançon, and U. Dahmen, Mater. Sci. Forum **294–296**, 27 (1999).
[21] F. Lançon, J. M. Penisson, and U. Dahmen, Europhys. Lett. **49**, 603 (2000).
[22] J. V. Barth *et al.*, Phys. Rev. B **51**, 4402 (1995).
[23] K. M. Ho and K. P. Bohmen, Phys. Rev. Lett. **59**, 1833 (1987).
[24] V. Rosato, M. Guillopé, and B. Legrand, Philos. Mag. A **59**, 321 (1989).
[25] M. Guillopé and B. Legrand, Surf. Sci. **215**, 577 (1989).
[26] T. Deutsch, P. Bayle, F. Lançon, and J. Thibault, J. Phys. Condens. Matter **7**, 6407 (1995).
[27] J. W. Cahn, Acta Metall. Mater. **39**, 2189 (1991).